SCIENTIFIC REPORTS

OPEN

SUBJECT AREAS:
ENVIRONMENTAL SCIENCES
ENVIRONMENTAL HEALTH

Received
18 July 2014

Accepted
11 November 2014

Published
2 December 2014

Correspondence and requests for materials should be addressed to D.A.M. (macleod@atm.ox.ac.uk)

Visualizing the uncertainty in the relationship between seasonal average climate and malaria risk

D. A. MacLeod[1] & A. P. Morse[2,3]

[1]Atmospheric, Oceanic and Planetary Physics, University of Oxford, [2]School of Environmental Sciences, University of Liverpool, [3]NIHR, Health Protection Research Unit in Emerging and Zoonotic Infections, Liverpool.

Around $1.6 billion per year is spent financing anti-malaria initiatives, and though malaria morbidity is falling, the impact of annual epidemics remains significant. Whilst malaria risk may increase with climate change, projections are highly uncertain and to sidestep this intractable uncertainty, adaptation efforts should improve societal ability to anticipate and mitigate individual events. Anticipation of climate-related events is made possible by seasonal climate forecasting, from which warnings of anomalous seasonal average temperature and rainfall, months in advance are possible. Seasonal climate hindcasts have been used to drive climate-based models for malaria, showing significant skill for observed malaria incidence. However, the relationship between seasonal average climate and malaria risk remains unquantified. Here we explore this relationship, using a dynamic weather-driven malaria model. We also quantify key uncertainty in the malaria model, by introducing variability in one of the first order uncertainties in model formulation. Results are visualized as location-specific impact surfaces: easily integrated with ensemble seasonal climate forecasts, and intuitively communicating quantified uncertainty. Methods are demonstrated for two epidemic regions, and are not limited to malaria modeling; the visualization method could be applied to any climate impact.

The link between climate and malaria is well studied[1–7]: rainfall and temperature influence the life cycles of the *Anopheles* mosquito vector and the malarial *Plasmodium* parasite. Malaria incidence shows a lagged correlation with precipitation[6,7], generally after a sustained rainfall there is a delay until malaria incidence increases in the human population.

To study the relationship between seasonal average climate and subsequent malaria risk, we use the Liverpool Malaria Model[8] (hereafter LMM). The model is driven by daily time series of temperature and precipitation and explicitly simulates the gonotrophic cycle of the Anopheles mosquito vector, the sporogonic cycle of the malaria parasite within the vector, and the interaction between vectors and human hosts (further details are given in the methodology).

Previous work with the LMM has shown skill when run in seasonal prediction mode for West Africa and southern Africa, using seasonal hindcasts produced from DEMETER and ENSEMBLES projects[9–11]. However the relationship between seasonally averaged climate and possible malaria outcomes is relatively unexplored. Here we consider this as a question of model response: by driving the malaria model with multiple temperature/rainfall time series and stratifying the output by the climate driver sharing the same average characteristics, we can discover the nature of the relationship between average climate states and malaria risk. That is, we can start to quantify the possible malaria outcomes possible given a mean seasonal average climate.

Temperature and precipitation time series from the 140 year 20th Century reanalysis[12] are used for this purpose. This data has been chosen for its long time series, to more fully explore the model response. No assertion here is made about its skill; as for this investigation it is only necessary that the daily evolution of temperature and precipitation is more realistic than an artificial time series.

In order to explore the uncertainty of the malaria model, key parts have varied between believable ranges, giving an idea of the sensitivity of the output to these parts. This method is inspired in part by standard ensemble techniques used climate modelling[13]. One such part as identified by users of the model is the equation used to describe the probability of survival of the mosquitos at each daily time step. Three formulations for this survival scheme based on empirical relationships in the literature are built into the model and are studied in this current work. Details of these schemes are given in the methodology, hereafter named schemes 1–3 for simplicity.

Results

Two regions are considered for analysis, both chosen for their unimodal rainfall seasonality. For each, ten grid points along the same latitude showing similar seasonal cycles are selected, to generate a larger ensemble of temperature and precipitation daily time-series. The first region covers part of the Sahel, at latitude 16.2°N and from −1.9° to 15°E, and the second is from southern Africa, at latitude 20°S and from 15° to 31.9°E. For each region, ten grid points across 140 years of reanalysis gives 1400 separate years of temperature and precipitation. Climatologies are shown in figure 1. The unimodal precipitation peak for both regions is related to the passing of the intertropical convergence zone and the temperature climatology is higher for the Sahelian region (fig. 1a) than southern African region (fig. 1b), due the higher latitude and increased rainfall in the latter region.

These 1,400 time series of daily mean temperature and daily rainfall are then used as input for the LMM. To do so the model is initialized with default values (e.g. for mosquito numbers) and 'spun-up' with one year of climatology for the region, which is appended onto the front of every year. This generates a realistic initial state appropriate the region, before simulating the effect on malaria dynamics of the temperature and precipitation for an individual year. Note that we consider the year for each region to start during the dry season when mosquito numbers are at their lowest; minimizing the impact of possible variability in initial conditions.

These 1,400 simulations are carried out three times, each time with a different survival scheme. Output climatologies are shown in figure 2 for the Sahel (results for southern Africa are contained in the supplementary material for brevity). The lagged response of malaria incidence is clear, with the season starting roughly two to three months following the start of the rainfall season. However, there is a large variation between the outputs when using the different mosquito survival schemes: significantly lower maximum incidence is simulated when using scheme 1 compared to the others, whilst the length of the transmission season varies between four months (figure 2a) and seven months (figure 2c). Similar variation in malaria seasonality between survival schemes is also seen for the southern African region (figure S1).

For each region a season is then defined, based on the period in the year experiencing the most rainfall (according to figure 1): June-September (JJAS) for the Sahel and December-March (DJFM) for southern Africa. A four-month malaria season is also defined, based on figures 2 and S1: September-December (SOND) for the Sahel and February-May (FMAM) for Southern Africa. These seasons are then used to calculate average climate and malaria incidence for each of the 1400 simulated years of reanalysis, which are then used to explore the relationship between seasonal average climate and malaria risk.

Malaria incidence can then be plotted as a function of average climate. This is achieved by subdividing climate space into 20 bins of equal interval in the temperature and precipitation dimensions.

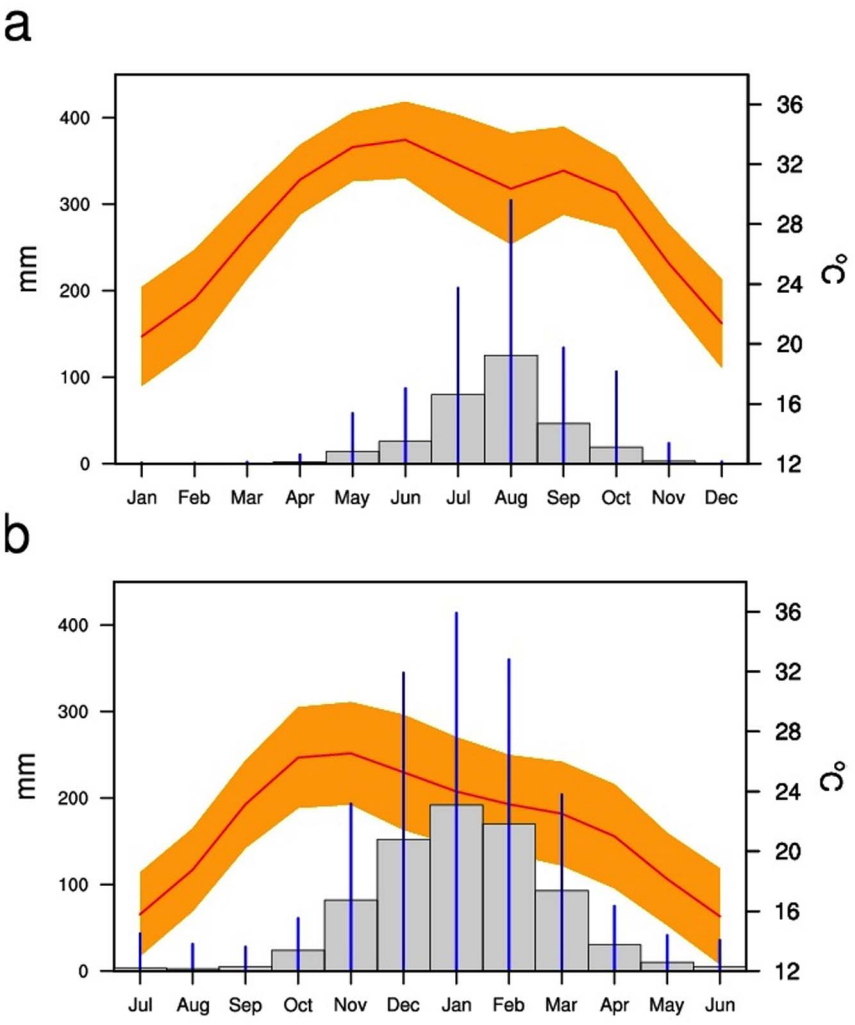

Figure 1 | Precipitation (blue) and temperature (orange) climatology for the Sahelian (a) and Southern African (b) regions. Error bars/shading indicates 5–95% range across all years and gridpoints.

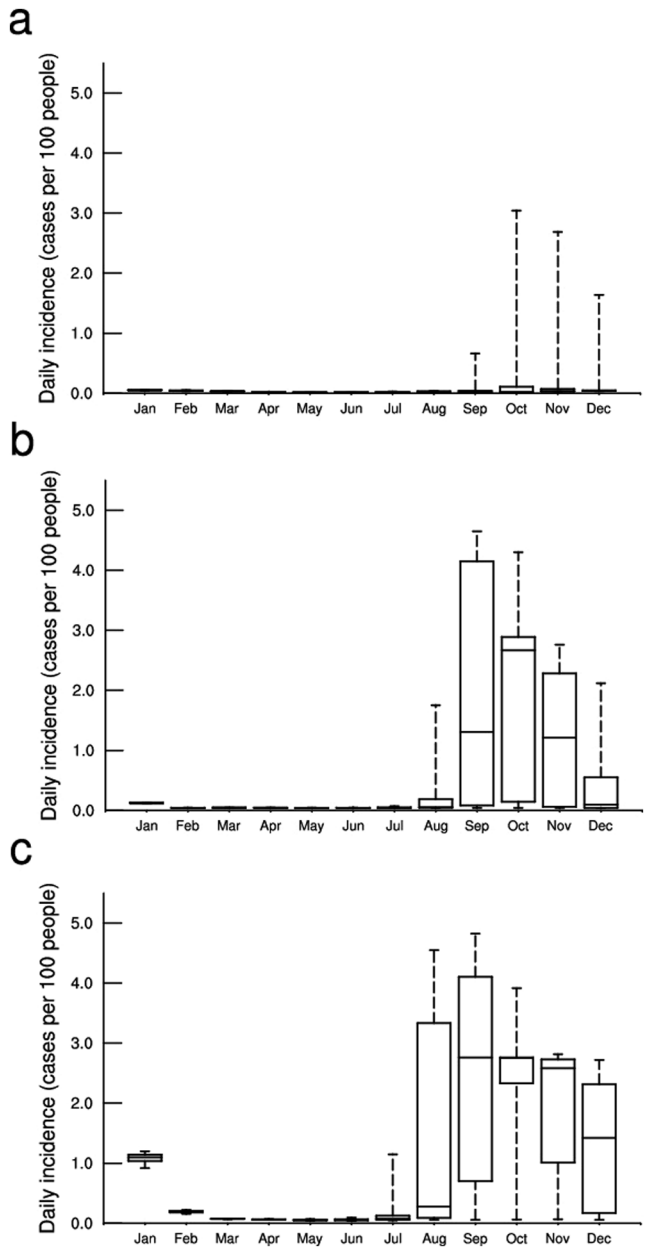

Figure 2 | Malaria incidence climatology over the Sahelian region, output from the LMM using survival schemes 1–3 (a–c). Details of survival schemes are given in the methodology section and results for Southern African region are shown in supplementary material.

Then for each bin mean and standard deviation incidence is calculated for the subset of the 1400 points falling within that bin. Looking at the mean gives an idea of the expected average malaria incidence following a season with a certain average climate, whilst the standard deviation indicates the variability of LMM behavior and gives a measure of the relative uncertainty of incidence associated with certain climate average states over others.

Results for the Sahel are shown in figure 3. The magnitude of the mean incidence (fig. 3a, c &e) varies significantly between the survival schemes, though is relatively highest for high precipitation states and lowest for low total precipitation. There is a large difference between the schemes when looking at the standard deviation of incidence.

For scheme 1 (fig. 3b) higher variation is seen for high precipitation states, with low variation when total precipitation is below 300 mm. Scheme 2 (fig. 3d) has the highest variability for states around 300 mm precipitation, whilst standard deviation for scheme 3 is highest when total precipitation is below 300 mm, and lowest when it is higher than 300 mm. This demonstrates the impact of model uncertainty, not just on the estimation of mean states but on estimates of uncertainty themselves. If a single survival scheme alone were used to assess the variation in malaria risk associated with a single average climate state, schemes 1 and 3 would give exactly opposing assessments (i.e. comparing fig. 3b and fig. 3f). This variability in model behavior with survival scheme illustrates the nonlinear effects of model uncertainty: survival schemes are a function of temperature alone and have no precipitation dependence, yet large differences in the model response to different precipitation totals are seen with different survival schemes. This is an important result when considered in conjunction with other uncertain parameters; whilst small uncertainties in their values may not seem relevant, the climate-malaria system is highly nonlinear and they may have a much larger impact than a simple analysis would suggest.

Corresponding figures for the southern African region are shown in the supplementary material (figure S2). Results are similar, in that the locations of maximum and minimum incidence are roughly similar between schemes, whilst the relative magnitudes are quite different. There are differences as well in the standard deviation plots between the schemes, though some regions in climate space with some agreement on the magnitude of the uncertainty. For example, all schemes simulate a low variability in incidence when the seasonal total precipitation is low, and show a high variability when the temperatures are high and rainfall is around 300 mm. However for rainfall totals around 600 mm, simulations using scheme 1 or 2 show a large variability in model response, whilst incidence simulated using scheme 3 shows low variability for average seasonal climates in this region.

The question of how this information might be combined has been considered, leading to the creation of impact surfaces. These allow a visualization of the relationship between seasonal average climate and simulated malaria risk. The first step was to simplify output based on tercile categories: 33rd & 67th percentiles are used to classify all of the 1,400 points as lower, middle or upper tercile (for each survival scheme separately). Each box in climate space is then classified into a certain malaria risk category according to the combined model response across all survival schemes.

The combination of information and selection of malaria risk categories is based on IPCC guidelines[14]. Recommendations to IPCC authors suggest that confidence in a result should be defined along two dimensions: amount and agreement of evidence. With these ideas in mind, any box with less than three members is classified as *"no strong warning"*, reflecting the idea that it is not appropriate to interpret any model result as a signal, when only a few integrations have been carried out.

Subsequently boxes with over 90% of points indicating upper tercile are initially classified as *"upper tercile very likely"*: of these, any box with less than ten members is downgraded to *"upper tercile likely"* (reflecting again the relationship between amount of evidence and confidence). Boxes with between 66–90% of points are then classified as *"upper tercile likely"*. The same procedure is applied for lower tercile events. Any remaining points, i.e. those with a majority of middle tercile events, or a majority of less than 66%, are defined as "*no strong warning*". Note that the choice of 66% and 90% and the terminology of *"likely"* and *"very likely"* are chosen for their direct correspondence to IPCC guidelines, whilst the three member and ten member thresholds relating to amount of evidence are arbitrary.

These rule-combined impact surfaces for both the Sahelian and the southern African region are shown in figure 4. For the Sahelian region (fig. 4a), there is clear separation between states related to high and low risk; when rainfall is low, malaria risk is very likely to be low, whilst high rainfall states are related to enhanced malaria risk. This is

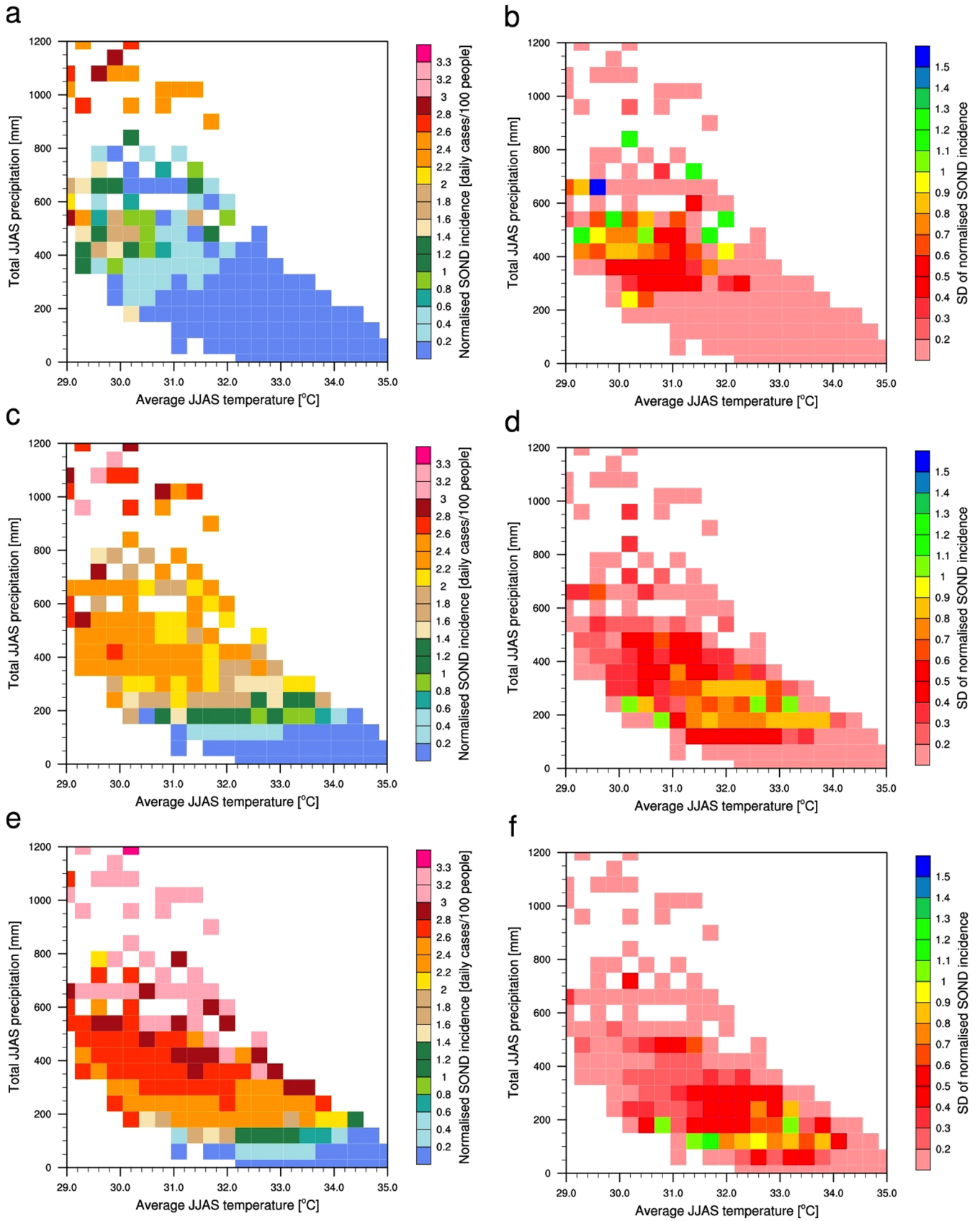

Figure 3 | Mean (a, c, e) and standard deviation (b, d, f) of malaria incidence for the Sahelian region, plotted in climate space, for survival schemes 1–3 (top to bottom). Results for Southern Africa are shown in supplementary material.

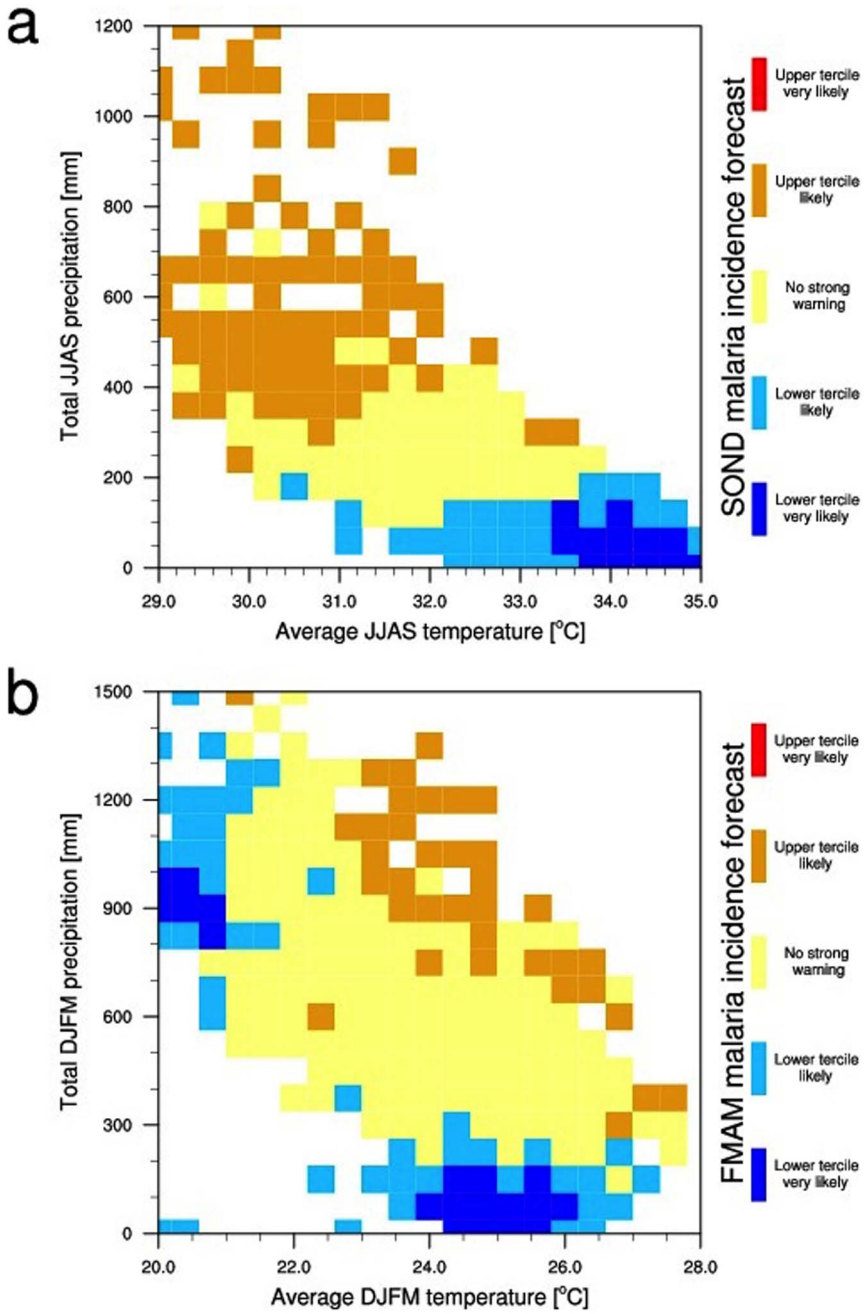

Figure 4 | Impact surfaces for the Sahelian (a) and Southern African (b) regions, combining malaria model output for all survival schemes.

in agreement with the fundamental dynamics, that is, the creation of mosquito breeding grounds by rainfall events.

For the southern African region, there are two regions in climate space associated with low malaria risk; low rainfall and low temperature states. The mechanism by which low rainfall creates low malaria risk is outlined above, whilst low temperature affects the relative life cycle of the vector and parasite. For instance, multiplication of the parasite within the vector is dependent on the sporogonic threshold: below 18°C no development occurs.

For both surfaces, there are no climate states giving a very likely upper tercile incidence, whilst certain climate states give a clear signal of lower tercile incidence. This suggests that certain climate states (e.g. drought, or cold average temperature) tend to lead more regularly to low risk malaria seasons than any particular climate state leads to a high-risk season.

Discussion

This work is an initial exploration and proof of concept, but we feel that these impact surfaces are an effective way of communicating the malaria risk and uncertainty due to climate drivers. Furthermore, they can be combined with an uncertain climate forecast by mapping individual forecast ensemble members to the surface. The forecast could be updated over time, and would eventually evolve into a single point as the precipitation season progresses and concludes.

Combining a seasonal climate prediction with an impact surface in this way would demonstrate the uncertainty in a climate-driven malaria forecast and its evolution over time. The relatively simple end product rests upon complex modeling and quantification of uncertainties, allowing effective communication of information related to forecast confidence. The method does not require any creation of a smoothed probability distribution function before

use: climate input can essentially be used raw. It would likely need bias correction, as the climate of a seasonal climate model will not be identical to reality.

There is an assumption about the inputs: that the daily time series of the reanalysis dataset employed is representative of reality. No analysis of the realism of the sub-seasonal variability and the distribution of rain days in the reanalysis has been carried out; it was used in an *ad hoc* manner. This assumption could be investigated by comparing the reanalysis to station data in relevant regions. The investigation could also be repeated by using synthetic data, generated for instance by a weather generator[15].

Whilst we have investigated one aspect of the malaria model uncertainty, other uncertainties remain unquantified. For example, our initial conditions for each year correspond to dry-season mosquito numbers calculated from a year of simulation with climatological rainfall and temperature. Variations in dry-season mosquito numbers could impact results, for instance if interventions completely reduced mosquito numbers to near zero it would be difficult for a subsequent rainfall to lead to an upper tercile rainfall season.

Interventions and other variability in initial conditions in mosquito numbers are outside the scope of this study. However we presume, based on timescales of the mosquito lifecycle and experience working with this particular model, that the impact of natural variability in dry-season mosquito numbers on eventual malaria outcome following the rainy season is quite small compared with the variability associated with interannual variation in subsequent temperature and rainfall.

As with any complex model there are many uncertain model parameters within the LMM, such as the human recovery rate and the mosquito maturing age, amongst many others. Exploration of the full model parameter space may well demonstrate sensitivity of the results to certain parameters, or robustness associated with others. There are also potentially relevant real-world aspects associated with malaria infection that are not included within the model, such as human immunity, which may also influence the results.

Despite this the survival scheme is one of the largest uncertainties in the model, and so this work provides a first order quantification of model uncertainty. This may be further refined by carrying out sensitivity testing of the malaria model to other parameters (similar to climate model perturbed parameter experiments). Co-varying parameters would also further explore the combined errors, working toward a goal of fully quantifying the uncertainty within this particular malaria model. The method would also easily allow the incorporation of additional weather-based malaria models[16,17], in a multi-disease model approach toward uncertainty quantification, such has been carried out in other studies[18,19]. It could also be easily applied to other sectors where seasonal climate has an impact, such as elsewhere within the health sector or for agricultural or energy forecasting.

Model uncertainty is just one uncertainty that a decision-maker needs to reckon with, and operationally must be considered in tandem with other factors. However a tailor-made visualization may help to simply communicate quantified key modeling uncertainties, and the work described here is the first step toward the creation of such a tool.

Methodology

The Liverpool Malaria Model (LMM). The LMM is a dynamic, process-based model driven by daily time-series of rainfall and temperature. A full description of the model can be found in the literature[8,20], a short summary follows here.

Both disease transmission and the mosquito population are modeled in the LMM. Model parameters are taken from the literature[21] such that the rate of development of the parasite within the mosquito (the sporogonic cycle, which takes place only above a threshold temperature of approximately 18°C) and the mosquito biting rate (the gonotrophic cycle, which has a threshold of approximately 9°C) are directly proportional to the heating degree days above the relevant threshold experienced by the mosquito.

In the absence of literature quantifying the relationship (and in place of a more complex hydrological model incorporating land-surface heterogeneity), the availability of surface water for mosquito breeding sites is simply modeled by fixing the eggs laid by each female mosquito to be proportional to the previous ten days' (dekadal) rainfall. Larval mosquito mortality rate is also dependent on dekadal rainfall.

Adult mosquito survival has three options for formulation, referred hereafter to as survival schemes. The first scheme is based on Martens et al.[22], which is a polynomial fitted to three data points. The daily survival is given by equation 1:

$$P = -0.0016T^2 + 0.054T + 0.45 \quad (1)$$

The second scheme is based upon Lindsay and Birley[23], and uses a fixed probability per gonotrophic cycle, given by equation 2:

$$P = exp\left(\frac{P_{lb}}{T_g}\right) \quad (2)$$

where P_{lb} is the model parameter for survival per cycle (given the value of 0.5, based on a range in the literature of 0.48–0.54[24–26]), and T_g is the gonotrophic cycle length at the current day.

The final scheme is based on Craig[27], which is an exponential function fitted to the same three points published by Martens. The survival probability for the Craig scheme is given by equation (3):

$$P = exp\left(\frac{-1}{-4.4 + 1.31T - 0.03T^2}\right) \quad (3)$$

Reanalysis data. The 20th Century reanalysis[18] spans 1871–2010 and assimilates only surface pressure reports, using observed monthly sea-surface temperature and sea-ice distributions as boundary conditions. Spatial resolution is 2.2° × 2.2° and it is available at a six hourly timestep.

1. Martens, P. *et al.* Climate change and future populations at risk of malaria. *Glob. Environ. Chang.* **9**, 89–107 (1999).
2. Lindblade, K. A., Walker, E. D., Onapa, A. W., Katungu, J. & Wilson, M. L. Highland malaria in Uganda: prospective analysis of an epidemic associated with El Niño. *Trans. R. Soc. Trop. Med. Hyg.* **93**, 480–487 (1999).
3. Thomson, M. C., Mason, S. J., Phindela, T. & Connor, S. J. Use of rainfall and sea surface temperature monitoring for malaria early warning in Botswana. *Am. J. Trop. Med. Hyg.* **73**, 214–21 (2005).
4. Loevinsohn, M. E. Climatic warming and increased malaria incidence in Rwanda. *Lancet* **343**, 714–718 (1994).
5. Briët, O. J. T., Vounatsou, P., Gunawardena, D. M., Galappaththy, G. N. L. & Amerasinghe, P. H. Temporal correlation between malaria and rainfall in Sri Lanka. *Malar. J.* **7**, 77 (2008).
6. Hashizume, M., Terao, T. & Minakawa, N. The Indian Ocean Dipole and malaria risk in the highlands of western Kenya. *Proc. Natl. Acad. Sci. U. S. A.* **106**, 1857–62 (2009).
7. Zhou, G. Association between climate variability and malaria epidemics in the East African highlands. *Proc. Natl. Acad. Sci.* **101**, 2375–2380 (2004).
8. Hoshen, M. B. & Morse, A. P. A weather-driven model of malaria transmission. *Malar. J.* **3**, 32 (2004).
9. Thomson, M. C. *et al.* Malaria early warnings based on seasonal climate forecasts from multi-model ensembles. *Nature* **439**, 576–579 (2006).
10. Jones, A. E. & Morse, A. P. Application and Validation of a Seasonal Ensemble Prediction System Using a Dynamic Malaria Model. *J. Clim.* **23**, 4202–4215 (2010).
11. Jones, A. E. & Morse, A. P. Skill of ENSEMBLES seasonal re-forecasts for malaria prediction in West Africa. *Geophys. Res. Lett.* **39**, L23707 (2012).
12. Compo, G. P. *et al.* The Twentieth Century Reanalysis Project. *Q. J. R. Meteorol. Soc.* **137**, 1–28 (2011).
13. Collins, M. Ensembles and probabilities: a new era in the prediction of climate change. *Philos. Trans. A. Math. Phys. Eng. Sci.* **365**, 1957–1970 (2007).
14. Mastrandrea, M. D. *et al. Guidance Note for Lead Authors of the IPCC Fifth Assessment Report on Consistent Treatment of Uncertainties. Intergovernmental Panel on Climate Change (IPCC)* Technical report, available at <http://www.ipcc.ch/pdf/supporting-material/uncertainty-guidance-note.pdf> (2010) Date of access:26/10/2014.
15. Richardson, C. W., Barrow, E. M., Semenov, M. A. & Brooks, R. J. Comparison of the WGEN and LARS-WG stochastic weather generators for diverse climates. *Clim. Res.* **10**, 95–107 (1998).
16. Ermert, V., Fink, A. H., Jones, A. E. & Morse, A. P. Development of a new version of the Liverpool Malaria Model. I. Refining the parameter settings and mathematical formulation of basic processes based on a literature review. *Malar. J.* **10**, 35 (2011).
17. Tompkins, A. M. & Ermert, V. A regional-scale, high resolution dynamical malaria model that accounts for population density, climate and surface hydrology. *Malar. J.* **12**, 65 (2013).

18. Caminade, C. *et al*. Impact of climate change on global malaria distribution. *Proc. Natl. Acad. Sci.* **111**, 3286–3291 (2014).
19. Ruiz, D. *et al*. Testing a multi-malaria-model ensemble against 30 years of data in the Kenyan highlands. *Malar. J.* **13**, 206 (2014).
20. Morse, A. P., Doblas-Reyes-REYES, F. J., Hoshen, M. B., Hagedorn, R. & Palmer, T. N. A forecast quality assessment of an end-to-end probabilistic multi-model seasonal forecast system using a malaria model. *Tellus A* **57**, 464–475 (2005).
21. Detinova, T. S. Age-grouping methods in Diptera of medical importance with special reference to some vectors of malaria. *Monogr. Ser. World Health Organ.* **47**, 13–191 (1962).
22. Martens, W., Jetten, T., Rotmans, J. & Niessen, L. Climate change and vector-borne diseases. *Glob. Environ. Chang.* **5**, 195–209 (1995).
23. Lindsay, S. W. & Birley, M. H. Climate change and malaria transmission. *Ann. Trop. Med. Parasitol.* **90**, 573–88 (1996).
24. Ansell, J., Hamilton, K. A., Pinder, M., Walraven, G. E. L. & Lindsay, S. W. Short-range attractiveness of pregnant women to Anopheles gambiae mosquitoes. *Trans. R. Soc. Trop. Med. Hyg.* **96**, 113–6 (2002).
25. Ferguson, H. M. & Read, A. F. Why is the effect of malaria parasites on mosquito survival still unresolved? *Trends Parasitol.* **18**, 256–261 (2002).
26. Charlwood, J. D. Survival rate variation of Anopheles farauti (Diptera: Culicidae) between neighboring villages in coastal Papua New Guinea. *J. Med. Entomol.* **23**, 361–5 (1986).
27. Craig, M. H., Snow, R. W. & le Sueur, D. A climate-based distribution model of malaria transmission in sub-Saharan Africa. *Parasitol. today* **15**, 105–11 (1999).

Acknowledgments

DM would like to acknowledge funding from a NERC PhD stipend, thank Francisco Doblas-Reyes (Institut Català de Ciències del Clíma - IC3) for a useful discussion of IPCC uncertainty, as well as personally thanking Cyril Caminade, Anne Jones and Andy Heath for support during the PhD. APM acknowledges funding from the European Union's Seventh Framework Programme projects; QWeCI (Quantifying Weather and Climate Impacts on health in developing countries, grant agreement 243964) and HEALTHY FUTURES (grant agreement 266327), and the Natural Environment Research Council Project End-to-End Quantification of Uncertainty for Impacts Prediction (EQUIP) NE/H003487/1.

Author contributions

D.M. conceived the idea, carried out the analysis and wrote the paper. The malaria model was provided along with PhD supervision and discussion of the paper by A.P.M.

Additional information

Supplementary information accompanies this paper at http://www.nature.com/scientificreports

Competing financial interests: The authors declare no competing financial interests.

How to cite this article: MacLeod, D.A. & Morse, A.P. Visualizing the uncertainty in the relationship between seasonal average climate and malaria risk. *Sci. Rep.* **4**, 7264; DOI:10.1038/srep07264 (2014).